Title
Developing Different Formats for Combining Aqueous Two-Phase Systems with Isothermal DNA Amplification

Author
Le, Nguyen Khoi

Publication Date
2019

Peer reviewed|Thesis/dissertation

UNIVERSITY OF CALIFORNIA

Los Angeles

Developing Different Formats for Combining Aqueous Two-Phase Systems with Isothermal DNA Amplification

A thesis submitted in partial satisfaction

of the requirements for the degree Master of Science

in Bioengineering

by

Nguyen Khoi Le

2019

ABSTRACT OF THE THESIS

Developing Different Formats for Combining Aqueous Two-Phase Systems with Isothermal DNA Amplification

by

Nguyen Khoi Le

Master of Science in Bioengineering

University of California, Los Angeles, 2019

Professor Daniel T. Kamei, Chair

Infectious diseases remain a public health concern worldwide. They severely impact resource-poor areas, where the top 10 causes of deaths include diarrhoeal diseases, HIV/AIDS, and tuberculosis. One gold-standard detection method for these infectious agents is nucleic acid amplification with the polymerase chain reaction (PCR). Unfortunately, its requirements for laboratory trained personnel and equipment prevent it from becoming a useful diagnostic tool at the point of care. To eliminate the need for a thermocycler, isothermal DNA amplification techniques were developed, but they cannot stand alone as complete diagnostic tools. They still require an extensive DNA preparation step prior to amplification. In addition, before it can be brought to an end-user, the entire detection scheme from sample preparation to end detection needs to be incorporated on a platform, with all of the reagents stored.

This thesis tackles the first aim by describing the development of an integrated method to extract, purify, and amplify DNA in one step using a micellar aqueous two-phase system (ATPS) with thermophilic helicase-dependent amplification (tHDA). This one-pot system was able to detect a target sequence from whole bacteria samples with cell concentrations as low as 10^2 colony forming units/mL. This is the first known application of an ATPS to isothermal DNA amplification.

For the second aim, this thesis describes the work that has been done so far as part of the initial step to the development of a fully-integrated nucleic acid testing device using a microfluidic platform. To avoid relying on the cleanroom for fabrication and external pumps for fluid flow in the chips, vacuum-driven chips were made from 3D-printed master molds for the first time. In addition, to our knowledge, we demonstrated the first dehydration of a full reaction set up for the recombinase polymerase amplification (RPA), including all of the enzymes and the primers but not the reaction activator magnesium acetate. The promising results will serve as a good starting point for our work in developing stand-alone diagnostic devices that can be used at the point of care and allow for a fully automated sample-to-result testing procedure.

The thesis of Nguyen Khoi Le is approved.

Benjamin M. Wu

Wentai Liu

Daniel T. Kamei, Committee Chair

University of California, Los Angeles

2019

This work is dedicated to my grandfather An, my mother Anne,

my sister Nguyen, and my late grandmother Khuong

Table of Contents

List of Figures

List of Tables

Acknowledgments

I would like to express my gratitude to Dr. Daniel T. Kamei for his guidance over the past few years. He is, first and foremost, an incredible research mentor and professor who has challenged me to grow every day as a researcher and engineer. Through meetings, presentations, and lectures, I learned how to think critically, apply knowledge from classes, and present my ideas clearly. In addition, Dr. Kamei is a valuable life mentor who has taught me the value of being able to make sacrifices and be responsible for our own choices. Without his mentorship, I cannot imagine where I would be today, and for that, I owe a great deal of my success to him.

Next, I would like to thank Sherine Cheung for her mentorship and patience during my time in the lab. She was not only a person who just showed me lab skills, but also someone who really devoted her time to make sure that I grew as a researcher. Through her rigorous training and high expectations, she taught me how to think as a scientist, be persistent, and be a valuable member of a research team. Also, she was very patient in working with me on improving my presentation skills. Lastly, Sherine looked after me when I needed help the most, especially when I started. Without her, I would not have had the incredible experience with the Kamei Lab and grow to be who I am today.

I also like to extend my special thanks to Garrett Mosley and Phuong Nguyen for their support when I first joined the lab. While they were not directly involved with my training or research project, they helped me persist through the difficult start and adapt to the team. Phuong was especially instrumental in my transition to the lab as he was able to use his own experiences to teach me what I would need to improve on in the future as I do research with the Kamei lab.

Next, I would like to thank everyone whom I got an opportunity to work with in the past few years. Kathryn Dern, Alison Thach, Samantha Cheng, Samantha Zhang, and Amy Han helped

train me and teach me, from day one, the standards that were expected from researchers in the Kamei Lab. Then, as a researcher, I was joined by many brilliant and hard-working teammates as we tackled different projects together: Sherine Cheung, Matthew Yee, Elizabeth Gomes, Chloe Wu, Christina Pearce, Vincent Wong, Joshua Keefe, Amir Dailamy, Eumene Lee, Justin Paek, Milad Azimi, So Youn Lee, Grace Emmel, and Eric Yang. Among them, I would like to specifically acknowledge Sherine Cheung, Matthew Yee, So Youn Lee, and Milad Azimi, for their collaboration on the projects that make this thesis possible.

In addition, I would like to thank Sherine Cheung, Matthew Yee, Daniel Bradbury, and Kensuke Hirota for making my graduate school experience worthwhile. Their work ethic inspired me to keep working hard every day, and most importantly, their presence made our office a place that felt like home. Thank you to all of the members of the Kamei Lab for their continuous support during my time in the lab, and for making this lab my family at UCLA for the past six years. I could always count on every lab member for support as I embarked on this challenging journey as a researcher, and without them, I could not learn as much as I could have today.

Last but not least, I would like to thank my family and friends. My friends, especially my roommate, have been incredibly understanding of the hours and my dedication as a researcher. They have always been there with me through the good and the bad and have helped make my UCLA experience an incredible one. Most importantly, I owe everything to my family. My grandfather, my mother, and my sister always looked out for my well-being throughout these years. They inspired me to be the best person that I could be and supported me in all of my endeavors. And to my grandmother, I would like to thank her for being an angel by my side – for showing me what it means to be a good human being with an incredibly kind heart, and for protecting me throughout my journey as she watched me all the way from heaven.

Parts of Chapter 1 and Chapter 2 of this thesis is a version of: S. F. Cheung, M. F. Yee, N. K. Le, B. M. Wu, and D. T. Kamei, "*A one-pot, isothermal DNA sample preparation and amplification platform utilizing aqueous two-phase systems*," Anal. Bioanal. Chem. 410 (2018) 5255-5263. D.T. Kamei was the director of research for this article. This work was supported by a grant from the UCLA School of Dentistry.

Chapter 1: Motivation and Background

1.1 Introduction

Infectious diseases are caused by pathogenic microorganisms, such as bacteria and viruses. Since the year 2000, even though infectious disease mortality rates have been declining, they still remain among the top 10 causes of deaths for the populations in low-income countries based on 2016 statistics.[1] Tuberculosis, a respiratory disease caused by the bacterium *Mycobacterium tuberculosis*, claimed the lives of 1.6 million people worldwide in 2017.[2] The human immunodeficiency virus (HIV), responsible for the acquired immunodeficiency syndrome (AIDS), still remains a large public health issue, affecting 37 million people on Earth, at the end of 2017.[3] Diarrhoeal disease is responsible for approximately 500,000 lives of children under the age of five around the world each year and remains the second leading cause of death for the population of this age, with *Escherichia coli* being one of the two most common causes.[4] Due to the public health issues that they cause, there exists a need to develop diagnostic tools that can quickly and accurately detect for pathogens.

One current gold standard method of detection is the nucleic acid amplification test (NAAT), which can be used to detect for genetic material of infectious agents in a patient sample. The greatest advantage of the NAAT is its potential for high specificity down to the nucleotide base level, since the genetic sequence is unique to each organism. Typically, the NAAT workflow involves three main steps (Figure 1.1). First, the DNA will be extracted from the cells via specialized cell lysis and purification kits. Then, it will be amplified via the polymerase chain reaction, or PCR, before being detected via gel electrophoresis. Because this standard workflow

for the NAAT requires expensive equipment, trained personnel, and also involves many liquid-handling steps, the complexity of the NAAT makes it difficult to be used in resource-poor settings. Unfortunately, it is also these developing countries that could currently benefit most from these early diagnosis assays. Therefore, there is a growing need for simple and inexpensive NAATs that can be used at the point of care.

Figure 1.1: Standard NAAT workflow.

1.2 Isothermal DNA Amplification Techniques

An alternative approach to PCR is the use of isothermal amplification techniques, which precludes the need for thermocyclers. One such method is loop-mediated isothermal amplification (LAMP), which relies on auto-cycling strand-displacement DNA synthesis that operates optimally at 60-65°C. While LAMP is specific and robust, it can be difficult to design, requiring 4-6 primers to implement.[5] For this reason, we decided to explore two other isothermal amplification techniques, known as thermophilic helicase-dependent amplification (tHDA) and recombinase polymerase amplification (RPA). For tHDA, it relies on the ability of the enzyme DNA helicase to unwind DNA and allow primers to bind to the template strands.[6] Meanwhile, for RPA, it is initiated when the recombinase proteins and oligonucleotides form primer complexes. Then, single strand binding proteins will come to stabilize the strand, and allow the recombinase to dissociate.[7] Since both techniques use mechanisms other than heat to separate DNA strands and make space for primers to bind to the templates, it allows both of them to occur at constant lower temperatures. Moreover, they are both simple to design, requiring only two primers for each reaction. They also

have demonstrated promising applications in diagnostics, and have been shown to be able to detect a number of infectious agents.[8–11]

1.3 Aqueous Two-Phase Systems (ATPSs)

These isothermal amplification methods still require extensive sample preparation and extraction steps when confronted with unprocessed cell samples. Thus, sample preparation remains a crucial component for successful amplification. Because these methods are labor-intensive and require lab equipment, there is growing interest in incorporating simple and equipment-free bioseparation alternatives.

Aqueous two-phase systems (ATPSs) represent a potential means for achieving upstream bioprocessing. An ATPS is a liquid-liquid extraction system made of components that will form two immiscible phases. Compared to traditional oil-water systems, an ATPS provides a mild environment for biomolecules and prevents denaturation, since both phases are comprised predominately of water.[12,13] It has been demonstrated that biomolecules can be partitioned extremely into one particular phase of the system, depending on the physical and chemical characteristics of the biomolecules of interest, such as charge, hydrophobicity, and size.[14–16] Moreover, ATPSs have the benefits of being scalable, lightweight, and affordable. Therefore, ATPSs have been widely used in large-scale biomolecule purification and extraction processes. Some examples include separating hydrophobic proteins from hydrophilic ones [17], proteins from viruses [18], or plasmid DNA from cell lysates [19].

While ATPSs have been traditionally used in large-scale bioseparations, our laboratory has demonstrated a novel use of the ATPS as a pre-concentration tool to improve the sensitivity of

small-scale, paper-based diagnostic tools. Specifically, biomolecules were concentrated via partitioning into one of the two phases of an ATPS prior to its application to the lateral-flow immunoassay (LFA). Using this pre-concentration step, the detection limit of the LFA was improved 10-fold.[20–22] Sensitivity could be further enhanced when biomarkers were partitioned extremely to the interface of an ATPS, where the volume is small relative to either phase of the system.[23] Similarly, an ATPS was also used to enhance the sensitivity and decrease the time-to-detection of a paper- based spot immunoassay.[24]

The integration of an ATPS as a tool to extract and purify DNA prior to tHDA amplification is described in Chapter 2 of this thesis.

1.4 Microfluidic Devices

As we continue to move forward in developing a point-of-care NAAT device, there is a need to find a suitable platform upon which the entire NAAT workflow can be performed. For that reason, we turned our attention to microfluidic devices. Within the channels of these devices, fluid can be moved from one compartment to the next, a feature that may allow us to design an automated NAAT workflow, where the DNA may be extracted in one chamber and then amplified in another. In addition, microfluidic devices can allow users to run tests with much less sample and reagent volumes, and they can be designed to be portable and disposable, which will allow them to serve as great point-of-care lab-on-a-chip tools.[25] Microfluidic devices have been developed to incorporate DNA amplification tests on its platform.[26–28] Unfortunately, multiple issues remain even with these promising developments.

To start, many of the chips rely on the use of syringe pump systems to drive fluid flow within these channels. This severely hinders the ability of these chips to be truly equipment-free at the point of care. To overcome this issue, we will be exploring a concept known as vacuum-driven flow [29] (Figure 1.2). This method relies on the characteristic of the polymer polydimethylsiloxane (PDMS) to be air-permeable.

In traditional chips, under standard fabrication and storage conditions (under ambient atmospheric pressure), the entire chip will be filled with air, presumably at 1 atm. As a result, when the liquid is dispensed into the input well, there is no pressure gradient to drive fluid flow unless an external pressure is applied. This is undesirable since that means that a pump will need to be incorporated in the device. In vacuum-driven chips, the chips are first stored in a vacuum environment (e.g., 0.3 atm). Then, when the user opens the vacuum sealed package, air at 1 atm will rush into the fluid channels (indicated in green and light blue in Figure 1.2) faster than it permeates through the entire chip, since the fluid channels are open to the outside environment. Since PDMS is air-permeable, the air in the fluid channels can escape through the PDMS into the vacuum channels. This movement will create a pressure gradient in the fluid channels to drive fluid flow after it is added to the input well.

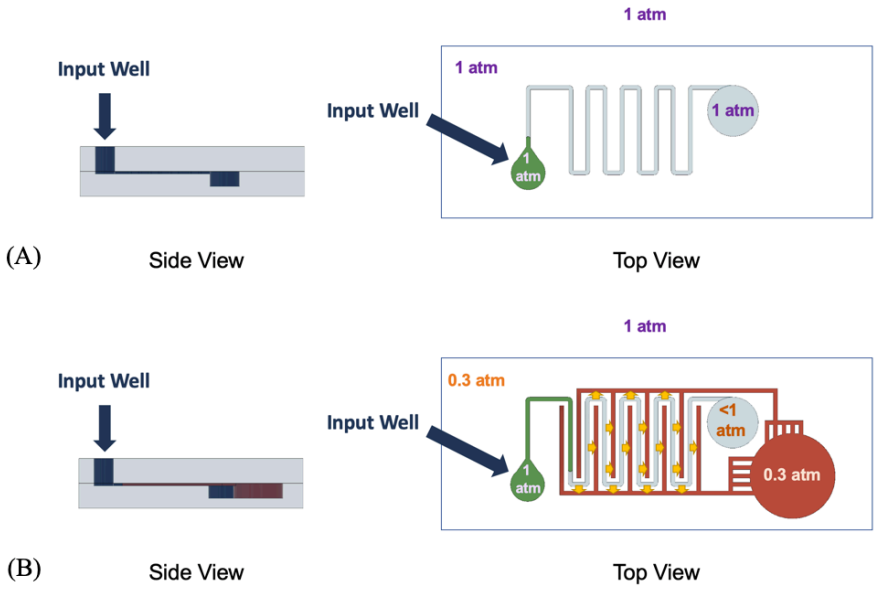

Figure 1.2: Vacuum-driven flow in PDMS chips. (A) In traditional chips, since the entire chip is at 1 atm, there is no pressure gradient to drive fluid flow unless an external pressure is applied. (B) In vacuum-driven chips, since only the fluid channels are open to the outside world while the rest of the chip is at a lower pressure condition, the air in the fluid channels can escape through the PDMS layer into the red vacuum channels. This movement will create a pressure gradient in the fluid channels to drive fluid flow.

The next issue with microfluidic devices is the master molds for these devices are often made via a lengthy process known as photolithography.[30,31] Since the cleanroom environment is an extremely limited resource and photolithography is an extensive process that requires training, this fabrication step can pose severe limitations to the process of research, development, and fabrication of these master molds. For this reason, 3D printing offers an attractive alternative to photolithography as a way to make these molds [32–34], and we used 3D printing to make our molds.

Finally, even though there has been research performed on integrating DNA amplification, more specifically the RPA, onto the microfluidic platform, it often requires a mixing step for the sample with the reagents prior to adding to the devices. This requirement will make the device less user-friendly. Unfortunately, while there are existing lyophilized RPA kits, they still require users to mix these pellets with a rehydration buffer, the sample (that may contain the DNA template of

interest), and the primers (that the users have to supply separately). To our knowledge, no one has yet to show a fully dehydrated RPA set up, where all of the reagents are dehydrated altogether (including primers), with the exception of the reaction activator magnesium acetate.

In Chapter 3 of this thesis, we will explore using 3D printing to make these vacuum-driven chips and also a method to dehydrate the RPA reagents altogether, and we will assess the amplification performance.

Chapter 2: A one-pot, isothermal DNA sample preparation and amplification platform utilizing aqueous two-phase systems

2.1 Introduction

In this study, we utilized an ATPS in conjunction with tHDA to develop a simplified NAAT diagnostic platform to detect for a model pathogen, *Escherichia coli* (*E. coli*) O157:H7. Our device uses a micellar ATPS composed of Triton X-100 surfactant as a means for extraction and concentration of DNA from whole cells. The released DNA could then be concentrated via partitioning into a single phase, and amplified without any additional user handling. Because the application of whole cells directly to the tHDA reaction has not been widely studied, we were also interested in testing the performance of our combined ATPS and tHDA platform, and comparing it to the tHDA reaction alone using unprocessed *E. coli* cell samples. To our knowledge, this is the first application of an ATPS as a platform technology for combining DNA sample preparation and isothermal DNA amplification. Moreover, a detection limit of 10^2 cfu/mL was achieved with our device. In this way, our unified platform – hereafter referred to as a one-pot reaction – addresses the traditional NAAT's limitation of being too complex by combining cell lysis, DNA extraction, and amplification processes into a single tube, while improving on the performance of existing tHDA technology.

2.2 Materials and Methods

2.2.1 Preparation of bacterial cell cultures

Escherichia coli O157:H7 strains (ATCC® 700728™) were cultured according to manufacturer protocol (ATCC, Manassas, VA) and plated onto Difco Nutrient Agar (Becton, Dickson and Company, Sparks, MD) plates. Cells were incubated at 37°C aerobically overnight. The plate was then sealed with Parafilm and stored at 4°C until use. Single colonies were picked from the agar plate and cultured in 5 mL of Difco Nutrient Broth (Becton, Dickson and Company, Sparks, MD) to prepare liquid bacterial culture. The cell suspension was then incubated in a shaker-incubator at 37°C and 240 rpm for 16 hours. To quantify bacteria concentrations within the suspension, OD 600 measurements were utilized, followed by plating serial dilutions of the bacteria culture. A standard curve to quantify the OD 600 measurements was produced by taking absorbance measurements of bacterial samples while concurrently plating them and counting the colonies after incubation. A standard curve was produced using samples with six absorbance measurements between 0.1 and 1.0. This standard curve was then used to determine bacteria concentrations for each reaction.

2.2.2 tHDA with purified genomic DNA and whole cells

Multiple pairs of primers were designed to target the *eae* gene found in *E. coli* O157:H7. All primer sequences were designed with the PrimerQuest Tool according to recommended parameters listed by the manufacturer, and obtained from Integrated DNA Technologies (Coralville, IA). Specifically, the suggested parameters include the primer size (24-33 bp), primer melting temperature (60-74°C, optimal 71°C), and primer G+C content (35-60%, optimal 44%), as well as the resulting amplified product size (80-120 bp, optimal 100 bp), melting temperature (68-75°C, optimal 71°C), and G+C content (optimal ~40%). Initial primer screening tests with

each primer pair were performed with purified genomic DNA extracted from overnight *E. coli* cultures using the Quick-gDNA Miniprep kit (Zymo Research). An 18 µL master mix solution of the tHDA reaction was prepared using IsoAmp® III Enzyme Mix (BioHelix, Beverly, MA), annealing Buffer II, $MgSO_4$, NaCl, IsoAmp® dNTPs, template DNA, and forward and reverse primers, according to manufacturer protocol. The amount of $MgSO_4$ was also varied to determine the optimal condition. After an optimal primer pair (Table 2.1) was identified, this primer pair and the manufacturer-prescribed reaction conditions were used as a starting point to perform tHDA with whole cells. For reactions with whole cells, the liquid bacteria culture was centrifuged at 12,000 rpm for 3 minutes to pellet the cells. The cells were then resuspended in the same volume of Nuclease Free Water (Coralville, IA), and 2.5 µL of the resuspension were added to the reaction. The remaining volume of the 50 µL reaction was filled with Nuclease Free Water, and the reaction was incubated on a heat block at 68°C for 60 minutes. A range of primer concentrations from 75 nM to 200 nM were tested in each reaction, upon which the optimal concentration of 150 nM was identified. The tHDA reactions with whole cells were then performed using the optimized primer concentration of 150 nM and manufacturer- suggested reaction conditions.

Forward primer	5′- TATCTACCGTCATATCCGGCATTAG -3′
Reverse primer	5′- GATTCGACTGCAGCTTATCAGAATTA -3′

Table 2.1: Forward and reverse primer sequences for the eae gene of E. coli O157:H7.

2.2.3 Preparation of Triton X-100 ATPS

For this study, a 100 µL Triton X-100 micellar ATPS with a top phase volume to bottom phase volume ratio of 1:1 was utilized. To ensure optimal conditions for the tHDA reaction, the concentrations of the Annealing Buffer II, $MgSO_4$, and NaCl in the ATPS were kept the same as

those in a regular tHDA reaction. The initial % w/w concentration of Triton X-100 (MP Biomedicals, Santa Ana, CA) was adjusted and optimized to obtain the desired equilibrium volume ratio of 1:1. Finally, Nuclease Free Water was added to a final volume of 100 µL.

To visualize the phase separation behavior of our system, 5 µL of 2% Brilliant Blue Dye FCF (The Kroger Co., Cincinnati, OH) were added to the mixed ATPS solution and vortexed thoroughly. The blue dye highlighted the micelle-rich bottom phase, while the micelle-poor top phase remained clear. After equilibrium phase separation was achieved, images before and after phase separation were captured with a Canon EOS 1000D camera (Canon U.S.A., Inc., Lake Success, NY) within a controlled lighting environment.

2.2.4 Determining partition coefficients of DNA in the one-pot reaction

Triton X-100 ATPSs with 1:1 volume ratios were prepared as previously described, with the ATPS components scaled to generate 200 µL ATPSs. 20 µL of annealing buffer, 16 µL of a 500 mM NaCl solution, and 8 µL of a 100 mM $MgSO_4$ solution were also incorporated to the ATPSs to mimic the conditions required for tHDA amplification. To each ATPS, either 200 ng of NoLimits 25 bp DNA fragment (Thermo Fisher), 200 ng of NoLimits 100 bp DNA fragment (Thermo Fisher), or 100 ng of O157:H7 *E. coli* genomic DNA were added. The genomic DNA for this study was obtained from liquid bacterial culture that had been incubated overnight as previously described, and extracted using the Quick-gDNA Miniprep kit (Zymo Research). Triplicate ATPSs were made for each type of DNA tested.

Upon phase separation, 10 µL were extracted from the top and bottom phases of each ATPS to be analyzed using the Quant-iT^{TM} High-Sensitivity dsDNA Assay Kit (Invitrogen). Each 10 µL of extracted sample was added to a 96-well plate with wells each containing 90 µL of a manufacturer-supplied buffer and fluorescent dye, which non-covalently binds to double-stranded

DNA. This dye is maximally excited at 502 nm, and its emission peak is at 523 nm when bound to DNA. The fluorescence intensity from each well is proportional to the concentration of DNA present in the solution. A standard curve was generated using DNA standards with known concentrations ranging from 0.2-100 ng of DNA. From this standard curve, a proportionality constant between DNA concentration and fluorescence intensity could be determined. However, since the presence of Triton X-100 surfactant can influence the fluorescence intensity, it was necessary to generate standards that account for surfactant concentrations corresponding to the top and bottom micelle-containing phases. Thus, for the micelle-poor and micelle-rich phases, 10 µL of either the top phase and bottom phase of a control ATPS containing no DNA were added to each DNA standard. The 96-well plate containing the DNA standards and samples was placed into a plate reader (TECAN Infinite F200) to quantify the fluorescence intensity. Once the standard curves were generated, the DNA concentrations from the top and bottom phase samples were then calculated using the respective acquired proportionality constants.

2.2.5 Amplification in the one-pot reaction

A 100 µL Triton X-100 ATPS with a volume ratio of 1:1 was prepared as previously described, with the exception that tHDA components were incorporated to implement amplification. Specifically, 10 µL of annealing buffer, 8 µL of a 500 mM NaCl solution, 6 µL of a 100 mM $MgSO_4$ solution, 7 µL of the dNTP solution, 4 µL of the enzyme mix, and forward and reverse primers were added to the ATPS. The reaction conditions were similarly optimized as with the tHDA-only reaction. A range of primer concentrations from 75 nM to 200 nM were tested, upon which the optimal concentration of 75 nM was identified. These components replaced equal amounts of water in the ATPS to achieve accurate volume ratios. To maintain equivalent cell concentrations between standard tHDA-only reactions and one-pot systems, 5 µL of an *E. coli*

suspension at various concentrations were added to the ATPS in place of water. The solution was then well-mixed via vortexing until the solution was clear and homogenous, after which the tube was heated at 68°C for one hour. Following heating, the ATPS was then analyzed for successful amplification of the target sequence.

2.2.6 Monitoring amplification in the one-pot reaction

Triplicates of the one-pot reaction were prepared as previously described. Upon mixing, the solution was heated at 68°C to allow for phase separation, DNA partitioning, and amplification. As the solution was heated, 5 µL sample volumes were carefully extracted with a micropipette from both the top and bottom phases. The phases were sampled every 15 minutes for 1 hour. Each 5 µL extracted sample was added to a 96-well plate containing 95 µL of a manufacturer-supplied buffer and SYBR Green I dye (Thermo Fisher). This dye is maximally excited at 497 nm, and its emission peak is at 520 nm when bound to DNA. The fluorescence intensity from each well is proportional to the concentration of DNA present in the solution. As previously described for the DNA partitioning studies, a standard curve was generated using DNA standards with known concentrations ranging from 0.2-100 ng of DNA (Invitrogen). Similarly, separate standards for the micelle-poor and micelle-rich phases were made by extracting 5 µL of either the top phase and bottom phase of a control Triton X-100 ATPS containing no DNA and adding it to each DNA standard. The 96-well plate containing the DNA standards and samples was placed into a plate reader (TECAN Infinite F200) to quantify the fluorescence intensity. Once the standard curves were generated, the DNA concentrations from the top and bottom phase samples were then calculated using the respective acquired proportionality constants.

2.2.7 Detection via gel electrophoresis

Detection of the target amplicon in both tHDA-only reactions and one-pot systems was conducted in two ways. First, initial analysis was performed via traditional gel electrophoresis and staining utilizing ethidium bromide. Briefly, a 50 µL 2% agarose (Promega) gel in Tris/Borate/EDTA buffer (Sigma) was prepared and mixed with 2.5 µL of a 10 mg/mL ethidium bromide (Bio-Rad) solution before cooling. Following amplification, either 10 µL of the micelle-poor top phase of the one-pot reaction or 10µL of the tHDA-only reaction were extracted. Each amplified sample was mixed with DNA 6x Loading Dye (Thermo Fisher Scientific) and pipetted into the wells of the gel. Similarly, 5 µL of O'GeneRuler Ultra Low Range DNA Ladder (Thermo Fisher Scientific) were loaded onto the gel as the standard to distinguish the size of the DNA product. The gel was immersed in Tris/Borate/EDTA buffer in a gel electrophoresis chamber (Mini-Sub® Cell GT Cell, Bio-Rad) connected to a PowerPac 200 power source (Bio-Rad), which was then run at 105 volts for 35 minutes. The gel was then removed and examined on a UV Transilluminator (UVP) under a 302 nm light for a target 100 bp band, indicating successful amplification. Gel images were subsequently captured with a Thermo Scientific™ myECL™ Imager. The 100 bp target band was then excised from the gel and purified using the PureLink™ Quick Gel Extraction Kit (Invitrogen). The purified sample was subsequently sent to Laragen, Inc (Culver City, CA) for sequencing.

2.3 Results and Discussion

2.3.1 Phase separation in the ATPS

A micellar ATPS composed of Triton X-100 surfactant was selected for the one-pot reaction. Specifically, Triton X-100 surfactant was ideal for several reasons. First, Triton X-100 is a

commonly used cell lysis agent. It has been previously demonstrated that, near and above the critical micelle concentration, Triton X-100 surfactant is able to solubilize membrane components, resulting in the disruption of cell membranes.[35] Thus, we anticipated that it would facilitate lysis of whole cells that are added to a mixed ATPS. Secondly, at and above the critical micelle concentration, the Triton X-100 surfactant monomers form micelles in aqueous solution, and phase separation can be induced by an increase in temperature. In concert with phase separation, biomolecules can be partitioned into one of the two phases, thereby resulting in their concentration. We anticipated that this concentration phenomenon could be exploited for the extraction and concentration of DNA from whole cells. Specifically, it was expected that DNA molecules released from the lysed cells would partition preferentially to the top, micelle-poor phase, where they experience fewer excluded-volume interactions with the smaller and less abundant micelles in that phase. Lastly, unlike polymer-salt ATPSs, in which one phase is salt-rich, the micellar ATPS does not require high salt concentrations for phase separation. Since we envisioned ultimately combining the ATPS purification directly with the isothermal tHDA reaction – which is sensitive to salt concentration – this characteristic was an important criterion in our ATPS selection.

A 1:1 volume ratio Triton X-100 ATPS was achieved with 9% w/w Triton X-100 and the appropriate salt concentrations for the tHDA reaction. Macroscopic phase separation was completed within 15 minutes of incubation at 68°C. The Triton X-100 ATPS forms a relatively more hydrophilic micelle-poor top phase and a denser, more hydrophobic micelle-rich bottom phase. Partitioning of biomolecules between the two phases is predominantly dependent on size, as well as relative hydrophobicity. Therefore, when Brilliant Blue FCF dye was added into the mixed ATPS, it partitioned extremely to the micelle-rich bottom phase due to its small size and

hydrophobicity. The addition of the dye thus yielded a blue bottom phase, while the top phase remained clear due to the absence of dye (Figure 2.1).

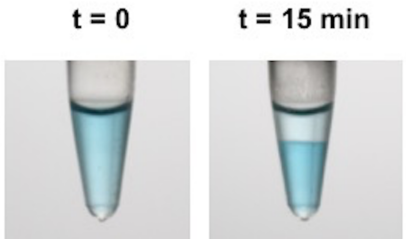

Figure 2.1: Phase separation in the Triton X-100 ATPS platform. At t=0, the ATPS is well-mixed, and Brilliant Blue FCF dye is dispersed throughout the entire solution. After incubation at 68°C, the ATPS phase separates into a clear micelle-poor top phase and a blue micelle-rich bottom phase containing the partitioned Brilliant Blue FCF dye.

2.3.2 DNA partitioning in the ATPS

Upon achieving a 1:1 Triton X-100 ATPS, it was necessary to assess the viability of the ATPS as a platform technology for sample preparation. Specifically, we verified that the DNA released from whole cells indeed partitioned to the micelle-poor top phase, as expected. We observed the partitioning behavior of three different types of DNA: a 25 bp DNA fragment, a 100 bp DNA fragment, and *E. coli* genomic DNA. The 25 bp DNA fragment and the 100 bp DNA fragment were chosen to model the partitioning behavior of the primers (~25 bp) and the expected tHDA product (100 bp), respectively. The average partition coefficients (concentration of DNA in the top phase divided by concentration of DNA in the bottom phase) for each DNA type are shown in Figure 2.2. For all three DNA types, the average partition coefficients were all greater than one, indicating that all three DNA types partition preferentially to the micelle-poor top phase. This was consistent with our hypothesis that the DNA should be driven to the top, micelle-poor phase due to experiencing greater repulsive, excluded-volume interactions with the larger and more abundant micelles in the bottom, micelle-rich phase. The average partition coefficient for the 25 bp DNA

fragment was found to be 3.81 ± 0.12. Meanwhile, the average partition coefficients of the 100 bp DNA fragment and genomic DNA were 23.2 ± 1.3 and 20.2 ± 3.4, respectively. This indicated that the 25 bp DNA fragment partitioned less extremely to the micelle-poor top phase than the 100 bp DNA fragment and genomic DNA. An explanation for this may be that the smaller 25 bp fragment experienced fewer excluded-volume interactions with the micelles in the micelle-rich bottom phase, which led to its less extreme partitioning into the micelle-poor top phase. In contrast, both the 100 bp DNA fragment and the genomic DNA yielded similar, larger partition coefficient values, likely due to their experiencing greater excluded volume interactions with the micelles in the bottom phase. Notably, the preferential partitioning of the DNA to the micelle-poor top phase results in its concentration in half the original volume. This is significant in that it confirmed that concentration of released genomic DNA can be achieved with the TX-100 ATPS, demonstrating its ability to serve as an appropriate sample preparation platform.

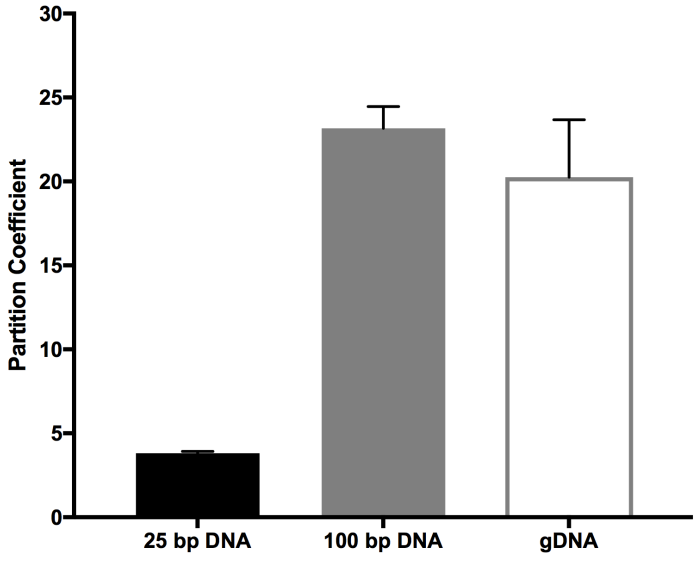

Figure 2.2: Average partition coefficients (n=3) of a model 25 bp DNA fragment, 100 bp DNA fragment, and genomic DNA (gDNA) in the one-pot reaction. The average partition coefficient for the 25 bp DNA fragment was found to be 3.81 ± 0.12. The average partition coefficients of the 100 bp DNA fragment and genomic DNA were 23.2 ± 1.3 and 20.3 ± 3.4, respectively.

2.3.3 Proposed mechanism for one-pot reaction

After verifying that the DNA released from whole cells indeed partitioned to the top micelle-poor phase of the TX-100 ATPS, we assessed the compatibility of the ATPS with the tHDA reaction. To do this, the one-pot reactions were set up as previously described, and various whole cell concentrations were directly added. DNA concentrations were measured in the top and bottom phases of a one-pot reaction every 15 minutes during the one-hour reaction time. Figure 2.3 shows the data from triplicate one-pot reactions at 10^6 cfu/mL, compared to triplicates of tHDA-only reactions at 10^7 and 10^6 cfu/mL. DNA concentration in the top phase of the one-pot reaction was significantly higher than that of the bottom phase within the first 15 minutes of incubation at 68°C and at all time points thereafter, which coincided with the expected DNA partitioning behavior. Furthermore, it is notable that the DNA concentration in the one-pot reaction at 10^6 cfu/mL was similar to that of the tHDA-only reaction containing a starting concentration of 10^7 cfu/mL. In contrast, the DNA concentration of the tHDA-only reaction containing 10^6 cfu/mL was significantly less than that of the one-pot reaction containing 10^6 cfu/mL. We also observed that just half the concentration of primers (75 nM) in the one-pot reaction was sufficient for amplification in the one-pot reaction, compared to 150 nM primers needed for the tHDA reaction alone. This indicated that the DNA concentration phenomenon we observed from the partitioning studies in the one-pot set-up can significantly improve DNA amplification outcomes.

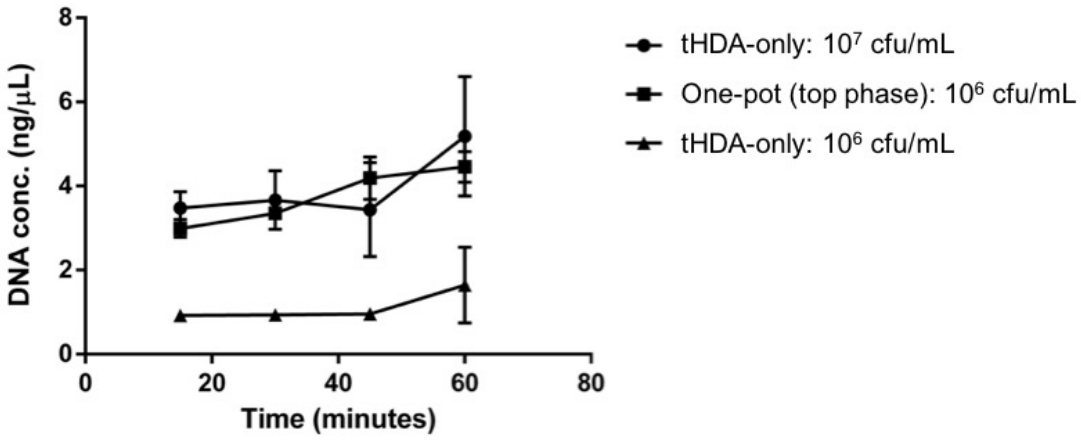

Figure 2.3: Comparison of DNA concentration over time in the one-pot reaction and the tHDA-only reaction (n=3). Use of the one-pot reaction with a starting cell concentration of 10^6 cfu/mL (squares) increases the DNA concentration such that it becomes comparable to the tHDA-only reaction with a 10^7 cfu/mL starting cell concentration (circles) at all time points measured.

Additionally, the DNA concentration in the top phase was found to increase over time, demonstrating that the helicase and polymerase enzymes in the tHDA reaction remained operational and were compatible with the Triton X-100 ATPS. Moreover, while DNA concentration increased in the top phase over time, it remained nearly constant in the bottom phase. This is an indication that not only does the DNA partition preferentially to the top phase, but that the tHDA amplification reaction also occurred in the top phase of the one-pot system. A possible explanation for this is that the helicase and polymerase enzymes involved in the tHDA reaction also partitioned preferentially to the top, micelle-poor phase; as such, DNA amplification occurred primarily in the top phase. These results helped to elucidate a proposed mechanism for the one-pot reaction (Figure 2.4), in which the cells are first lysed, the DNA partitions within the first 15 minutes, and is then predominately amplified in the top phase during the remainder of the 1-hour reaction time.

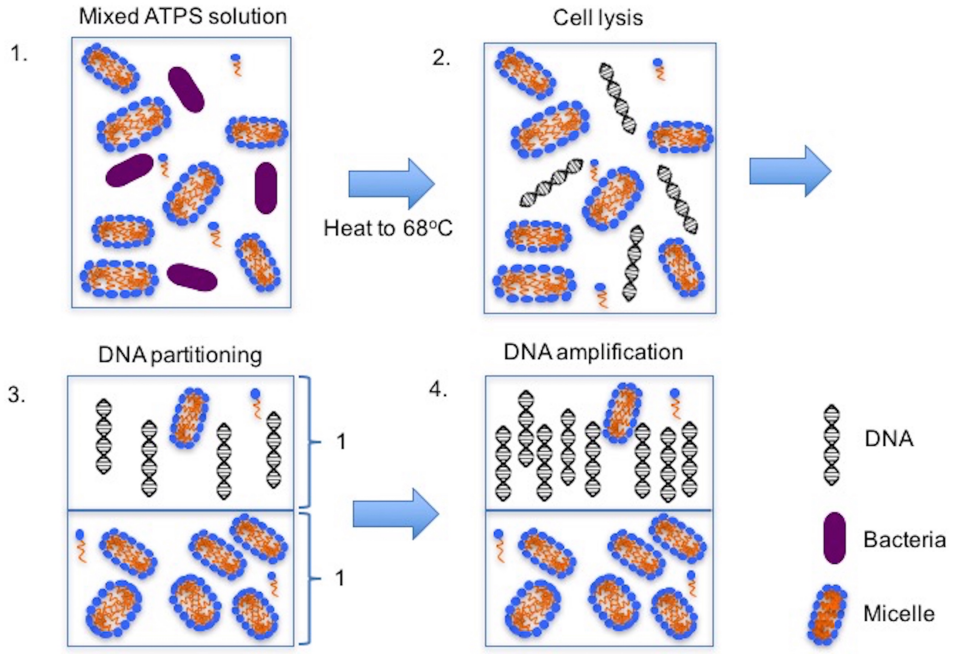

Figure 2.4: Proposed mechanism for the one-pot reaction. 1) Whole cells are added into a one-pot reaction containing Triton X-100 and tHDA reagents for amplification. 2) The mixture is incubated at 68°C, and the cells become lysed by the Triton X-100 surfactant and heat, allowing the DNA to be released. 3) Phase separation is achieved, and the DNA released from the cells is partitioned to the top phase of the ATPS. 4) The DNA is amplified and collected in the top phase of the one-pot reaction.

2.3.4 Determining the limit of detection of the one-pot system

After identifying a potential mechanism for the one-pot reaction, we then wanted to determine the detection limit of the one-pot reaction. To do this, the one-pot reaction was tested with a range of whole cell concentrations, using the optimized reaction conditions for the one-pot reaction. For comparison, these cell concentrations were similarly tested with the conventional tHDA reaction alone, using the optimized reaction conditions for the tHDA-only reaction with whole cells. Gel electrophoresis was used to determine whether the target DNA sequence was successfully amplified (Figure 2.5). The amplified product was expected to be 100 bp long; thus, the appearance of a 100 bp band in the gel indicated that the correct sequence was amplified. Using

the tHDA reaction alone, it was determined that amplification could be achieved at an initial cell concentration of 10^7 cfu/mL. Meanwhile, when the cell concentrations were decreased, amplification was no longer successful. Comparatively, when the one-pot reaction was tested, amplification was possible at initial cell concentrations as low as 10^4 cfu/mL. In fact, the 100 bp band is present even at concentrations as low as 10^2 cfu/mL, although smaller primer artifacts start to appear dominant. We believe that this is due to insufficient template genomic DNA being available to be amplified at these lower cell concentrations. Regardless, a significant improvement in the whole cell detection limit is observed using the one-pot reaction.

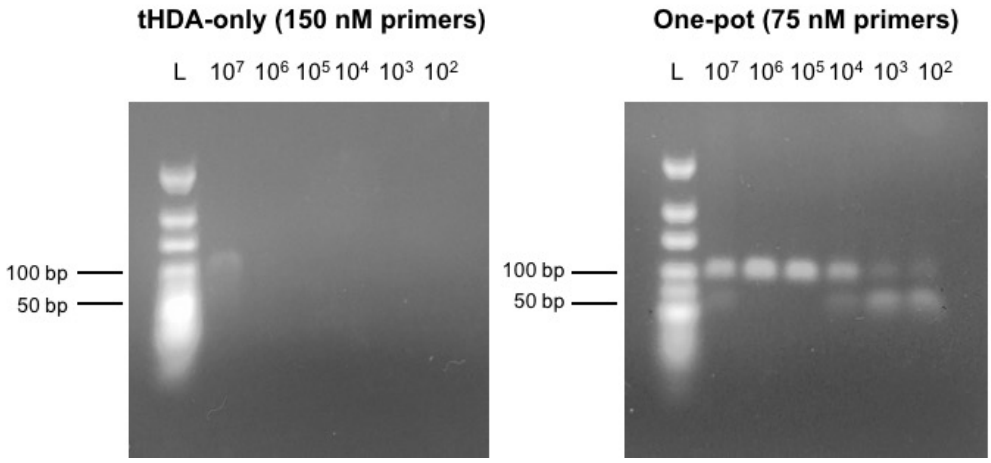

Figure 2.5: Gel electrophoresis comparison of DNA amplification from whole-cell samples in the one-pot reaction and in the conventional tHDA reaction. The numbers above the wells are in cfu/mL. The one-pot reaction is able to detect as low as 10^2 cfu/mL, although the 50 bp primer artifacts start to become dominant due to insufficient template genomic DNA at low cell concentrations.

The improvement in detection limit using the one-pot system can be further elucidated when we consider the proposed mechanism of the one-pot reaction, as discussed in Section 2.3.3 (Figures 2.3 and 2.4). Specifically, we compared the tHDA-only reactions performed with 10^7 and 10^6 cfu/mL with a one-pot reaction performed using 10^6 cfu/mL. When the one-pot reaction was

performed using 10^6 cfu/mL, DNA concentrations throughout the reaction were comparable to those of the tHDA-only reaction with 10^7 cfu/mL, meaning that the one-pot reaction sufficiently concentrated the released genomic DNA to a point where it could be amplified as effectively as if the initial starting cell concentration was 10 times higher. This outcome was similarly reflected in the gel electrophoresis data, where we confirmed that the one-pot reaction was able to detect and amplify from whole cell concentrations of 10^6 cfu/mL and lower. Sequencing results also allowed us to verify that the 100 bp product that was amplified in the one-pot reaction was indeed the exact sequence of the *eae* gene we expected (Figure 2.6).

Figure 2.6: Bi-directional sequencing verification of amplified product with the forward primer (a) and the reverse primer (b). The sequencing results yielded an exact match of the expected eae gene segment.

While we recognize that the current standard NAAT detection limit can be even lower when used with a commercially purified DNA sample, the emphasis of the development of the one-pot system is on the combination of cell lysis, DNA purification and extraction, and amplification all in one automated reaction. Moreover, it should be noted that research articles that have reported lower detection limits using isothermal technology utilized DNA samples that had undergone separate purification steps prior to amplification, or quantified genomic DNA that was purchased from a vendor.[36,37] In contrast, our studies focused on utilizing unprocessed, whole cells as our starting point. Moreover, the cell lysis, DNA extraction, and amplification are achieved within the same reaction volume, thus bypassing the need for separate compartments or pump-driven liquid transfer between multiple microfluidic chambers in chip-based devices.[38]

We believe that the substantial improvement of amplification from whole cell samples with the one-pot reaction can be attributed to several factors. While the DNA partitioning phenomenon in the one-pot reaction is responsible for the concentration of DNA in the top phase, we anticipate a synergistic effect that involves the purification of the DNA sample in the one-pot reaction as well. It was noted that when the tHDA-only reaction and the one-pot reaction were tested with genomic DNA that was extracted and purified with a commercial kit, the detection limits appear more similar (Figure 2.7). Although the one-pot reaction was still able to detect lower concentrations of template DNA, the disparity between the detection limits of the one-pot and tHDA-only reactions were not as drastic as when they were tested with whole cells. Considering that tHDA-only amplifies and detects DNA comparably to the one-pot reaction when the template DNA is purified, we believe that this points to tHDA's hindered activity in the presence of cell debris, such that amplification from whole cells is only possible when the cell concentration is sufficiently high. This further indicates that the one-pot reaction – via incorporation of the ATPS

– allows for a degree of DNA sample purification such that detection and amplification from whole cell samples is much improved. Thus, the DNA concentration and simultaneous purification via ATPS plays a crucial role in the success of the one-pot reaction.

	Number of template DNA copies
L	ladder
1	30,000
2	3,000
3	300
4	30

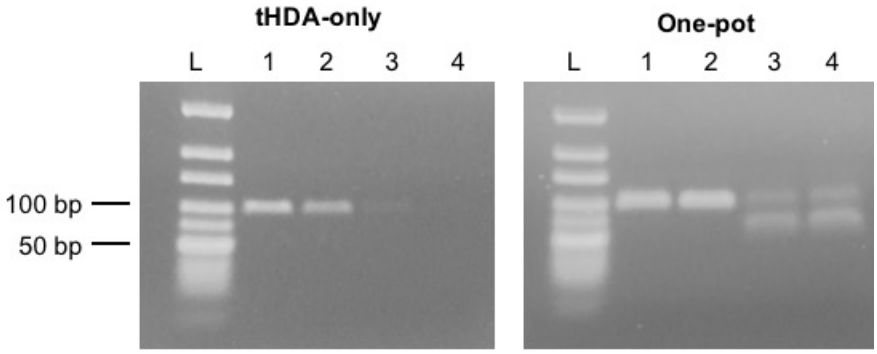

Figure 2.7: Gel electrophoresis comparison of DNA amplification from purified genomic DNA in the one-pot reaction and in the conventional tHDA reaction. The detection limits of both reactions are similar, although the one-pot reaction can detect as few as 30 copies of template DNA. 50 bp primer artifacts start to appear as the template DNA concentration becomes lower.

Our research group has also previously demonstrated that the use of a 1:1 volume ratio ATPS results in a two-fold concentration of large hydrophilic biomolecules, since the large hydrophilic biomolecules would partition extremely to one phase – half the original volume.[15,20,21] However, it is worth noting that in this study, the lowered detection limit that was achieved with the one-pot reaction utilizing a 1:1 ATPS exceeded the expected 2-fold improvement. One possible explanation may be that the two-fold increase in DNA concentration in the top phase of the ATPS sufficiently increased the number of interactions the DNA has with the reagents for amplification. As the number of interactions increase, DNA amplification can be more easily initiated, resulting in a multiple-fold improvement in the detection limit.

Alternatively, molecular crowding has previously been found to help improve DNA amplification efficiency.[39] To take advantage of this phenomenon, researchers have explored the use of enhancer additives, such as betaine, Ficoll, polyethylene glycol, and dextran, to simulate a crowding effect that has been demonstrated to promote amplification.[40] We hypothesize that using the one-pot system where the reaction is performed in the top phase may likewise simulate this crowding effect, and contribute to the overall improvement in the detection limit.

2.4 Conclusion

In summary, we successfully designed a novel NAAT platform that combines both sample preparation steps and subsequent amplification within a micellar ATPS. Moreover, the detection limit of the one-pot reaction using whole cells was found to be as low as 10^2 cfu/mL, a substantial improvement from the whole-cell detection limit of the existing tHDA technology (10^7 cfu/mL). Of note is that this improvement in detection limit was achieved with the automation of cell lysis, DNA extraction, and amplification in a single reaction volume. The viability of the direct addition of unprocessed samples to a one-step, sample-to-detection platform allows NAAT diagnostics to move towards eliminating upstream sample processing and multi-chamber chip-based platforms. Thus, this device embodies a simplified NAAT, where the user can directly add cell samples to the ATPS platform and perform amplification without any additional liquid handling. This platform is the first known application of ATPS with isothermal DNA amplification. While we demonstrated the functionality of our device using a model pathogen *E. coli* O157:H7, this platform technology can be modified by changing the primer sequences to detect specific DNA from other pathogens, making it a flexible and powerful diagnostic tool.

Chapter 3: Moving Towards a Fully-Integrated Point-of-Care Nucleic Acid Amplification Microfluidic Chip

3.1 Introduction

As we continue on our path to develop point-of-care nucleic acid amplification tools, we hope to design a final device that allows for sample-in-result-out to maximize user-friendliness. To do this, the device will need to (a) be able to move fluid on its own and (b) have all of the necessary reagents dehydrated onto its platform. For this reason, we investigated microfluidic chips for their ability to run automated lab tests using small volumes of samples. For now, we envision the final version of our chip to be comprised of two different zones. After the user puts in the sample, the sample will flow through the first zone where DNA will be extracted and prepared. Subsequently, the purified DNA solution will flow to and stay in the second zone, where the DNA will be amplified and detected. (Figure 3.1).

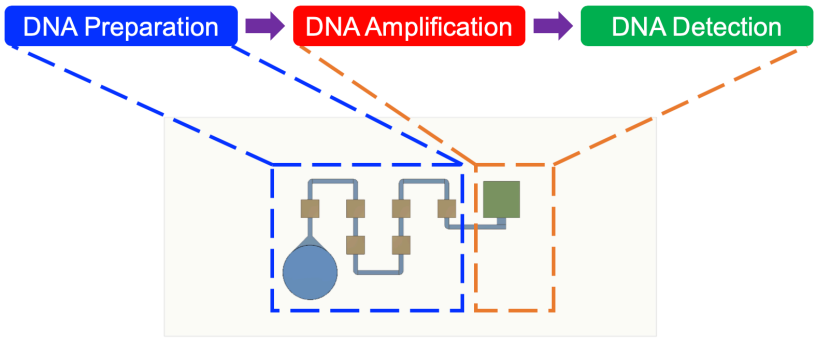

Figure 3.1: General overview of the vision for a final device. In this device, a microfluidic chip will have an an input well (light blue) and then a DNA preparation zone where DNA will be extracted and purified (blue dashed box), followed by a reaction chamber where DNA will be amplified and detected (orange box).

To proceed toward the final device, we fabricated microfluidic chips, ran the RPA reaction on the polymer layer, and explored a potential dehydration method for the RPA reagents. To our knowledge, this is the first time that a vacuum-driven microfluidic chip has been fabricated from a 3D-printed master mold. Meanwhile, though there are existing lyophilized RPA kits available, users will need to mix the rehydration buffers with the pellet, along with supplying their own primers. This mixing step can limit the user-friendliness of the device. In moving towards a user-friendly device, we will also show, for the first time, a successful full RPA reaction (with all of the necessary components, except magnesium acetate) dehydrated altogether in a tube format.

In the studies in this chapter, all DNA amplification reactions were performed with purified DNA for proof-of-concept. We will incorporate additional DNA preparation methods onto our microfluidic devices in the next iterations of the models.

3.2 Materials and Methods

3.2.1 Preparation of Purified DNA Samples

Escherichia coli O157:H7 strains (ATCC® 700728™) were cultured according to manufacturer protocol (ATCC, Manassas, VA) and plated onto Difco Nutrient Agar (Becton, Dickson and Company, Sparks, MD) plates. Cells were incubated at 37°C aerobically overnight. The plate was then sealed with Parafilm and stored at 4°C until use. To prepare bacterial suspensions for use in spot tests, single colonies were picked from the agar plate and cultured in 5 mL of Difco Nutrient Broth (Becton, Dickson and Company, Sparks, MD). The cell suspension was then incubated in a shaker-incubator at 37°C and 240 rpm for 16 h. Genomic DNA was

extracted using the *Quick*-DNA™ Miniprep Kit, following the manufacturer's protocol (Zymo Research, Irvine, CA).

3.2.2 Fabrication of Microfluidic Chips

Two models of the microfluidic chips were designed (Figure 3.2). These chips were comprised of two polydimethylsiloxane (PDMS) layers. The first chip was fabricated specifically for the purpose of studying flow inside a vacuum-driven chip (Figure 3.2A). It had an input well (4 mm (D) x 5 mm (H)), a final chamber (6 mm (D) x 3 mm (H)), and a vacuum storage chamber (10 mm (D) x 3 mm (H)). The fluid and vacuum channels were 500 µm in height and width. Meanwhile, the second chip was fabricated to run the RPA reaction on the PDMS layer (Figure 3.2B). It contained a reaction chamber that was big enough to hold a 50 µL reaction (4 mm x 4 mm x 2 mm) and an input well for sample dispensing (4 mm (D) x 5 mm (H)).

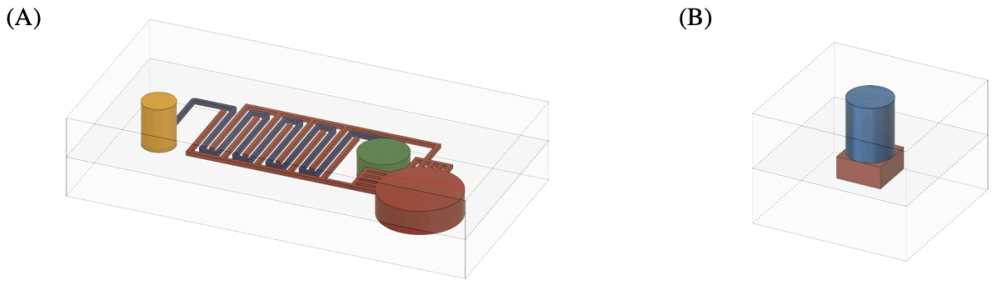

Figure 3.2: Fusion 360™ CAD drawings of the microfluidic chips. (A) The vacuum-driven chip designed for flow studies had an input well (yellow), a final chamber (green), a fluid system that connected those two components (blue), and a system of vacuum channels (red). (B) A chip fabricated specifically for running the RPA reaction on a PDMS layer contained a reaction chamber (red) and an input well for sample dispensing (light blue).

The master molds for these chips were designed using Fusion 360™ software (Autodesk, San Rafael, CA) and printed with acrylonitrile butadiene styrene (ABS) via a homemade 3D

printer. A layer of PDMS (10:1 w/w ratio for prepolymer to curing agent; Sylgard 184; Dow Corning, Midland, MI) was then cast using those molds. The PDMS was cured via baking in an oven at 70ºC for at least 3 h. Subsequently, the layers of the chips were cut and peeled from the molds before they were irreversibly bound to each other using an oxygen plasma machine (Harrick Plasma) to complete the chip fabrication. Finally, heavy weights were applied on top of the fabricated chips for at least 1 h to enhance bonding between the two layers.

3.2.3 Flow Study in the Vacuum-Driven Chip

After the vacuum chips were fabricated, a vacuum pump was used to draw air out from these chips. They were then stored inside a vacuum chamber at -70kPa for at least 3 h. When the chips were ready for testing, they were removed from the vacuum environment. Subsequently, 60 µL of a water solution, containing a diluted amount of Brilliant Blue Dye FCF (The Kroger Co., Cincinnati, OH) for visualization, was added to the input well. A video of the flow was recorded using an iPad (Apple, Cupertino, CA).

3.2.4 In-Tube and On-Chip RPA Reactions

Primers were designed to target the *eae* gene found in *E. coli* O157:H7 and obtained from Integrated DNA Technologies (Coralville, IA). The sequences for the optimal primers pair can be found in Table 3.1. The dNTPs were purchased from Thermo Fisher Scientific (Waltham, MA).

The RPA reaction was prepared and run according to manufacturer protocol for the TwistAmp® Liquid Basic Kit (TwistDx, United Kingdom), with slight modifications. In short, for a 50 µL reaction, 25 µL of 2x Reaction Buffer, 8 µL of dNTPs, 5 µL of 10x Basic E-mix, 2.5 µL of 20x Core Reaction mix, and 2 µL of each primer were first mixed together. For positive tests, 1 µL of the solution containing purified DNA was then added. Subsequently, Nuclease Free Water

(IDT, Coralville, IA) was used to adjust the volume of the solutions to 47.5 µL, before adding 2.5 µL of a 280 mM magnesium acetate solution to activate the reaction. All solutions were prepared in the 0.2 mL tubes with flat caps (Thermo Fisher Scientific, Waltham, MA) incubated on ice. For the reactions performed on PDMS layers, 50 µL of the abovementioned solution was added to the reaction chamber (shown in Figure 3.2B), and the top of the well was sealed with a piece of Parafilm to prevent materials exchange with the outside environment. The in-tube and on-chip reactions were incubated on a heat block at 39°C for 30 min before they were stored on ice again to stop the reaction. Finally, the results were analyzed via gel electrophoresis.

Forward primer	5′-CACTGGACTTCTTATTACCGTTCTATGATTCC-3′
Reverse primer	5′-GCGCCACCAATACCTAAACGGGTATTATCACC-3′

Table 3.1: Forward and reverse primer sequences for the eae gene of E. coli O157:H7.

3.2.5 RPA Reagent Dehydration Experiments

The RPA reagents were dehydrated in amounts suitable for 25-µL DNA amplification reactions. To do this, a 25 µL solution was prepared in the 0.2 mL flat-cap tubes and contained the RPA reagents at the appropriate concentrations: 12.5 µL of 2x Reaction Buffer, 4 µL of dNTPs, 2.5 µL of 10x Basic E-mix, 1.25 µL of 20x Core Reaction mix, 1 µL of each primer, and 2.75 of Nuclease Free Water. Next, the tubes were put in the -20°C freezer for at least 2 h. Subsequently, they were quickly transferred to a lyophilizer, where the frozen pellet was dried for at least another 2 h.

Finally, the freeze-dried pellets were rehydrated with 25 µL of solution. For positive tests, the solution contained 4.20 µL of the original purified DNA stock, 1.25 µL of a 280 mM

magnesium acetate solution, and 19.60 µL of Nuclease Free Water. Meanwhile, for negative tests, it only consisted of 1.25 µL of a 280 mM magnesium acetate solution and 23.75 µL of Nuclease Free Water. Our controls for the dehydration studies were 25 µL of non-dehydrated RPA reactions that contained 12.5 µL of 2x Reaction Buffer, 4 µL of dNTPs, 2.5 µL of 10x Basic E-mix, 1.25 µL of 20x Core Reaction mix, 1 µL of each primer, 1.25 µL of a 280 mM magnesium acetate solution, 1 µL of purified DNA stock (for positive test only), and Nuclease Free Water. The reactions were incubated on a heat block at 39ºC for 30 min before they were stored on ice to stop the reaction.

3.2.6 Detection via Gel Electrophoresis

Detection of the amplified target amplicon was conducted via traditional gel electrophoresis and staining utilizing ethidium bromide. Briefly, a 25-mL 2% agarose (Promega, Madison, WI) gel in Tris/Borate/EDTA buffer (Sigma Aldrich, St. Louis, MO) was prepared and mixed with 1.25 µL of a 10 mg/mL ethidium bromide (Bio-Rad, Hercules, CA) solution before cooling. Following amplification, 10 µL of each amplified sample was mixed with DNA 6× Loading Dye (Thermo Fisher Scientific, Waltham, MA) and pipetted into the wells of the gel. Similarly, 5 µL of GeneRuler Low Range DNA Ladder (Thermo Fisher Scientific, Waltham, MA) was loaded onto the gel as the standard to distinguish the size of the DNA product. The gel was immersed in Tris/Borate/EDTA buffer in a gel electrophoresis chamber (Mini-Sub® Cell GT Cell, Bio-Rad) connected to a PowerPac 200 power source (Bio-Rad), which was then run at 80 V for 45 min. The gel was then removed and examined on a UV Transilluminator (UVP, Upland, CA) under a 302-nm light for a target band slightly above 200 bp, indicating successful amplification.

3.3 Results and Discussion

3.3.1 Flow Study in the Vacuum-Driven Chip

To test if our chip fabricated from a 3D printed mold could move fluid on its own due to the vacuum, we added a solution containing dye into our device (Figure 3.3). After the liquid was dispensed into the input well, it traveled from the input well to the final well within 4 minutes, which indicates a reasonable flow rate within the device. While it might take a little longer to finish filling up the well (> 7 minutes), the size of the well is currently not designed for RPA reactions. Thus, the time-to-load might be different than what we observed here, and the flow rate could be further fine-tuned by changing other design parameters such as the distance between sample loading well and the final well.

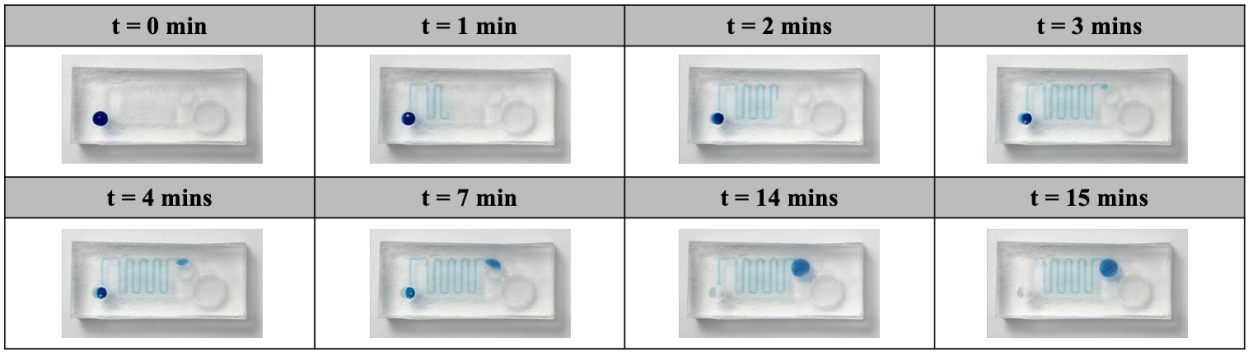

Figure 3.3: Flow of fluid in the vacuum-driven chip. The fluid was able to reach the final well in less than 4 minutes.

This result demonstrates the potential to fabricate vacuum-driven chips via 3D-printed molds. This is significant for two reasons. First, the vacuum-driven chip would allow for automated fluid flow within the channels, which can lead to automated lab testing and increased user-friendliness of the device. Second, the 3D printing process can allow the master molds of the chips to be fabricated outside of cleanrooms. This not only can lead to an increase in the production

of the chips themselves due to an increase in the availability of the master molds, but also allows for more active research in this field because it is easier to build a 3D printer than to build and maintain a cleanroom environment.

3.3.2 RPA Reaction on a PDMS Layer

This preliminary experiment examined if RPA reactions could be successful on PDMS layers. We had two in-tube tests (positive and negative) and two on-chip tests (positive and negative). The band of the target amplified product was expected to be slightly above the 200 bp mark. In both positive reactions, there was a bright target DNA band present, indicating successful amplification. For the negative tests, streakiness was observed, and we have found that the RPA reactions sometimes yields this type of streakiness. There was no glaring false positive present in these conditions since there was no bright DNA band (with good contrast in intensity to the rest of the bands) that was the same size as the target band. We do acknowledge the presence of more primer artifacts in these on-chip reactions, but this preliminary result is still promising as it demonstrated successful DNA amplification on a PDMS layer using the RPA reaction.

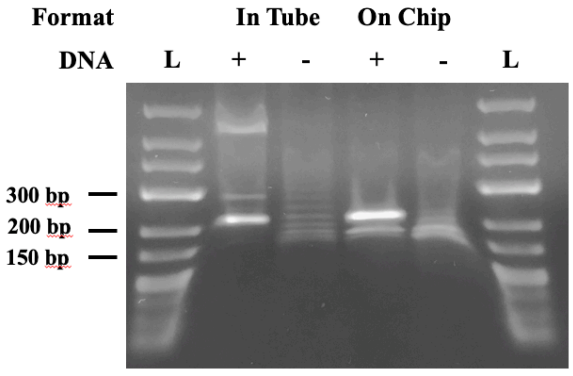

Figure 3.4: Gel electrophoresis comparison of in-tube and on-chip RPA reactions. The text at the top of the figure indicates whether the test was performed in the 0.2 mL flat-cap tube or in the PDMS reaction chamber and whether or not the test contained DNA. The on-chip RPA reactions yielded comparable results to that of the in-tube reactions.

3.3.3 Performance of Dehydrated RPA Reagents

We explored lyophilization as a potential dehydration method for the RPA reagents. All reactions were performed in tubes since we wanted to isolate the effect of dehydration. In this case, we dehydrated all RPA reagents together, except the activator magnesium acetate. In addition, since an advantage of microfluidic devices is their ability to use smaller volumes, we explored dehydration using smaller volumes of RPA reactions (more specifically, 25 μL). After we obtained the freeze-dried pellet, we resolubilized the pellet with a solution containing magnesium acetate (plus DNA if it was a positive test) and compared the results with the appropriate in-tube controls.

For the positive tests, both the control and dehydrated experiments yielded the bright correct bands of the appropriate size of slightly above 200 bp. This signal intensity was in clear contrast to the intensity obtained from the same base pair lengths in the negative tests (Figure 3.5). As a result, we have demonstrated that lyophilization is a promising dehydration method for our RPA reagents, including primers, as it was able to preserve enzymatic activity, indicated by successful amplifications seen in the positive tests. The next logical experiment to move forward after this study is to dehydrate the RPA reagents onto the PDMS platform using lyophilization.

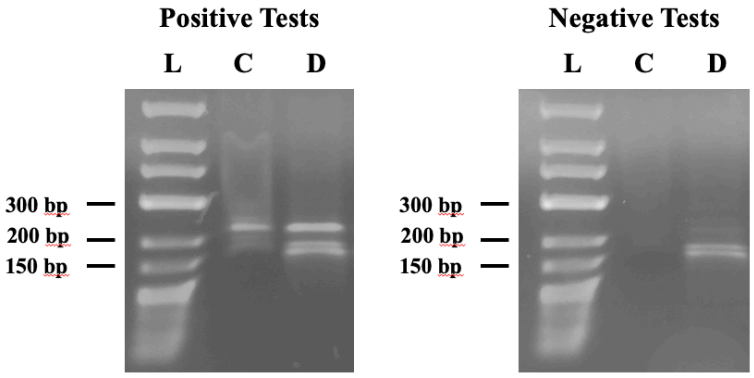

Figure 3.5: Gel electrophoresis results for the dehydration experiments. The left gel corresponds to the results from running positive RPA reactions (with DNA). The right gel corresponds to the results from running negative RPA reactions (without DNA). The lanes marked with the letter "C" depict the result from the control non-dehydrated reagent experiments, while the lanes marked with the letter "D" depict the result from the experiments with the dehydrated RPA reagents. We observed successful DNA amplification in both positive tests with little to no false positives obtained for the negative conditions.

3.4. Conclusions

In this project, we have laid out some first steps in the process of moving towards a fully automated point-of-care nucleic acid microfluidic chip. We began the project by first demonstrating successful fabrication of vacuum-driven chips from a 3D printed mold. This result is promising for two reasons. The 3D printing aspect will allow the process of research, development, and fabrication of microfluidic chips to be accessible to more users. Second, the vacuum-driven flow can allow us to design devices that can move fluid from one compartment to the next and allow for an automated testing procedure.

Next, we showed successful DNA amplifications on the PDMS surface using RPA as the first step of integrating this isothermal amplification method onto our device. Finally, we used lyophilization to successfully dehydrate the RPA reagents, including the primers but without magnesium acetate. While this last result was obtained in tubes, it is still a significant step forward

because if the reagents can all be dehydrated, then the users only have to add the sample to run the test instead of having to mix the sample with other solutions prior to using the device.

Moving forward, we hope to continue our dehydration studies by having the RPA reagents directly dehydrated onto the PDMS surface. As we continue to incorporate additional DNA preparation and detection methods onto our device, we are excited for the prospect of developing a fully automated, sample-in result-out microfluidic chip that can be used at the point of care for the detection of pathogenic DNA.

Bibliography

1. World Health Organization. The top 10 causes of death. *World Health Organization* (2018). Available at: https://www.who.int/news-room/fact-sheets/detail/the-top-10-causes-of-death. (Accessed: 11th June 2019)
2. World Health Organization. Tuberculosis. *World Health Organization* (2018). Available at: https://www.who.int/en/news-room/fact-sheets/detail/tuberculosis. (Accessed: 11th June 2019)
3. World Health Organization. HIV/AIDS. *World Health Organization* (2018). Available at: https://www.who.int/en/news-room/fact-sheets/detail/hiv-aids. (Accessed: 11th June 2019)
4. World Health Organization. Diarrhoeal disease. *World Health Organization* (2017). Available at: https://www.who.int/en/news-room/fact-sheets/detail/diarrhoeal-disease. (Accessed: 11th June 2019)
5. Notomi, T. *et al.* Loop-mediated isothermal amplification of DNA Tsugunori. *Nucleic Acids Res.* **28**, (2000).
6. Cao, Y., Kim, H. J., Li, Y., Kong, H. & Lemieux, B. Helicase-dependent amplification of nucleic acids. *Curr. Protoc. Mol. Biol.* 15.11.1-15.11.12 (2013). doi:10.1002/0471142727.mb1511s104
7. Piepenburg, O., Williams, C. H., Stemple, D. L. & Armes, N. A. DNA detection using recombination proteins. *PLoS Biol.* **4**, 1115–1121 (2006).
8. Boyle, D. S. *et al.* Rapid detection of Mycobacterium tuberculosis by recombinase polymerase amplification. *PLoS One* **9**, 1–9 (2014).
9. Boyle, D. S., Lehman, D. A. & Lillis, L. Rapid Detection of HIV-1 Proviral DNA for Early Infant Diagnosis Using Rapid Detection of HIV-1 Proviral DNA for Early Infant Diagnosis. *MBio* **4**, e00135-13 (2013).
10. Torres-Chavolla, E. & Alocilja, E. C. Nanoparticle based DNA biosensor for tuberculosis detection using thermophilic helicase-dependent isothermal amplification. *Biosens. Bioelectron.* **26**, 4614–4618 (2011).
11. Chow, W. H. A. *et al.* Application of isothermal helicase-dependent amplification with a disposable detection device in a simple sensitive stool test for toxigenic Clostridium difficile. *J. Mol. Diagnostics* **10**, 452–458 (2008).

12. Schütte, H. Protein purification by aqueous two-phase systems. in *Protein Structure Analysis* 31–48 (Springer Berlin Heidelberg, 1997). doi:https://doi.org/10.1007/978-3-642-59219-5_3

13. Albertsson, P.-A. *Partition of cell particles and macromolecules: sep- aration and purification of biomolecules, cell organelles, mem- branes, and cells in aqueous polymer two-phase systems and their use in biochemical analysis and biotechnology*. (Wiley, 1986).

14. Fisher, D. The separation of cells and organelles by partitioning in two-polymer aqueous phases. *Biochem. J.* **196**, 1–10 (1981).

15. Mashayekhi, F., Meyer, A. S., Shiigi, S. A., Nguyen, V. & Kamei, D. T. Concentration of mammalian genomic DNA using two-phase aqueous micellar systems. *Biotechnol. Bioeng.* **102**, 1613–1623 (2009).

16. Nikas, Y. J., Liu, C. L., Srivastava, T., Abbott, N. L. & Blankschtein, D. Protein Partitioning in Two-Phase Aqueous Nonionic Micellar Solutions. *Macromolecules* **25**, 4797–4806 (1992).

17. Quina, F. H. & Hinze, W. L. Surfactant-mediated cloud point extractions: An environmentally benign alternative separation approach. *Ind. Eng. Chem. Res.* **38**, 4150–4168 (1999).

18. Kamei, D. T., King, J. A., Wang, D. I. C. & Blankschtein, D. Separating lysozyme from bacteriophage P22 in two-phase aqueous micellar systems. *Biotechnol. Bioeng.* **80**, 233–236 (2002).

19. Ribeiro, S. C., Monteiro, G. A., Cabral, J. M. S. & Prazeres, D. M. F. Isolation of plasmid DNA from cell lysates by aqueous two-phase systems. *Biotechnol. Bioeng.* **78**, 376–384 (2002).

20. Mashayekhi, F. *et al.* Enhancing the lateral-flow immunoassay for viral detection using an aqueous two-phase micellar system. *Anal. Bioanal. Chem.* **398**, 2955–2961 (2010).

21. Mashayekhi, F., Le, A. M., Nafisi, P. M., Wu, B. M. & Kamei, D. T. Enhancing the lateral-flow immunoassay for detection of proteins using an aqueous two-phase micellar system. *Anal. Bioanal. Chem.* **404**, 2057–2066 (2012).

22. Jue, E., Yamanishi, C. D., Chiu, R. Y. T., Wu, B. M. & Kamei, D. T. Using an aqueous two-phase polymer-salt system to rapidly concentrate viruses for improving the detection limit of the lateral-flow immunoassay. *Biotechnol. Bioeng.* **111**, 2499–2507 (2014).

23. Chiu, R. Y. T., Thach, A. V., Wu, C. M., Wu, B. M. & Kamei, D. T. An aqueous two-phase system for the concentration and extraction of proteins from the interface for detection using the lateral-flow immunoassay. *PLoS One* **10**, 1–14 (2015).

24. Cheung, S. F. *et al.* A Combined Aqueous Two-Phase System and Spot-Test Platform for the Rapid Detection of Escherichia coli O157:H7 in Milk. *SLAS Technol.* **23**, 57–63 (2018).

25. Oblath, E. A., Henley, W. H., Alarie, J. P. & Ramsey, J. M. A microfluidic chip integrating DNA extraction and real-time PCR for the detection of bacteria in saliva. *Lab Chip* **13**, 1325–1332 (2013).

26. Ahrberg, C. D., Manz, A. & Chung, B. G. Polymerase chain reaction in microfluidic devices. *Lab Chip* **16**, 3866–3884 (2016).

27. Zhang, H. *et al.* LAMP-on-a-chip: Revising microfluidic platforms for loop-mediated DNA amplification. *TrAC - Trends Anal. Chem.* **113**, 44–53 (2019).

28. Dao, T. N. T. *et al.* A microfluidic enrichment platform with a recombinase polymerase amplification sensor for pathogen diagnosis. *Anal. Biochem.* **544**, 87–92 (2018).

29. Xu, L., Lee, H., Jetta, D. & Oh, K. W. Vacuum-driven power-free microfluidics utilizing the gas solubility or permeability of polydimethylsiloxane (PDMS). *Lab Chip* **15**, 3962–3979 (2015).

30. Yeh, E.-C. *et al.* Self-powered integrated microfluidic point-of-care low-cost enabling (SIMPLE) chip. *Sci. Adv.* **3**, 1–12 (2017).

31. Leester-Schadel, M., Lorenz, T., Jurgens, F. & Richter, C. *Fabrication of Microfluidic Devices*. *Microsystems for Pharmatechnology: Manipulation of Fluids, Particles, Droplets, and Cells* (2016). doi:10.1007/978-3-319-26920-7

32. Ho, C. M. B., Ng, S. H., Li, K. H. H. & Yoon, Y. J. 3D printed microfluidics for biological applications. *Lab Chip* **15**, 3627–3637 (2015).

33. Waheed, S. *et al.* 3D printed microfluidic devices: Enablers and barriers. *Lab Chip* **16**, 1993–2013 (2016).

34. Amin, R., Knowlton, S., Hart, A., Yenilmez, B. & Ghaderinezhad, F. 3D-printed microfluidic devices. (2016).

35. Partearroyo, M. A., Ostolaza, H., Goni, F. M. & Barbera-Guillem, E. Surfactant-Induced Cell Toxicity and Cell Lysis: A Study Using B16 Melanoma Cells. *Biochem. Pharmacol.* **40**, 1323–1328 (1990).

36. Du, X. jun, Zhou, T. jiao, Li, P. & Wang, S. A rapid Salmonella detection method involving thermophilic helicase-dependent amplification and a lateral flow assay. *Mol. Cell. Probes* **34**, 37–44 (2017).

37. Linnes, J. C., Rodriguez, N. M., Liu, L. & Klapperich, C. M. Polyethersulfone improves isothermal nucleic acid amplification compared to current paper-based diagnostics. *Biomed. Microdevices* **18**, 30 (2016).

38. Mahalanabis, M., Do, J., Almuayad, H., Zhang, J. Y. & Klapperich, C. M. An integrated disposable device for DNA extraction and helicase dependent amplification. *Biomed. Microdevices* **12**, 353–359 (2010).

39. Mok, E., Wee, E., Wang, Y. & Trau, M. Comprehensive evaluation of molecular enhancers of the isothermal exponential amplification reaction. *Sci. Rep.* **6**, 37837 (2016).

40. Tong, Y., Lemieux, B. & Kong, H. Multiple strategies to improve sensitivity, speed and robustness of isothermal nucleic acid amplification for rapid pathogen detection. *BMC Biotechnol.* **11**, 50 (2011).